

# Space-Time-Frequency Coded Multiband UWB Communication Systems

W. Pam Siritwongpairat, Weifeng Su, Masoud Olfat, and K. J. Ray Liu  
Department of Electrical and Computer Engineering and Institute for Systems Research,  
University of Maryland, College Park, MD 20742.

**Abstract**—In this paper, we propose a general framework to analyze the performance of multiband UWB-MIMO systems regardless of specific coding schemes. A combination of space-time-frequency (STF) coding and hopping multiband OFDM modulation is also proposed to fully exploit all of the available spatial and frequency diversities, richly inherent in UWB environments. We quantify the performance merits of multiband UWB-MIMO systems in case of Nakagami- $m$  frequency-selective fading channels. We show that the maximum achievable diversity of the proposed system is the product of the number of transmit and receive antennas, the number of multipath components, and the number of jointly encoded OFDM blocks. Interestingly, theoretical result shows that the diversity gain does not severely depend on the fading parameter  $m$ . Finally, simulation results are presented to support the theoretical analysis.

## I. INTRODUCTION

Ultra-wideband (UWB) is an emerging technology that offers great promises to satisfy the growing demand for low cost and high-speed digital wireless home networks. A traditional UWB technology is based on single-band approaches that directly modulate data into a sequence of impulse-like waveforms, which occupy the available bandwidth of 7.5 GHz. Recently, multiband UWB schemes were proposed in [1], in which the UWB frequency band is divided into several subbands, each with a bandwidth of at least 500 MHz in compliance with the FCC regulations. To efficiently capture the multipath energy, orthogonal frequency division multiplexing (OFDM) technique has been used to modulate the information in each subband. The major difference between multiband OFDM and traditional OFDM schemes is that the multiband OFDM symbols are not continually sent on one frequency-band; instead, they are interleaved over different subbands across both time and frequency.

In conventional RF technology, multiple-input multiple-output (MIMO) has been well known for its effectiveness of improving system performance in fading environment. Space-time (ST) codes have been proposed for narrowband communications, where the fading channel is frequency-non-selective. When the fading is frequency-selective, space-frequency (SF) coded MIMO-OFDM systems [2] have been shown to be an efficient approach to make benefits of spatial and frequency diversities. Recently, space-time-frequency (STF) codes (see [3] and references therein) have also been proposed for MIMO-OFDM systems. By utilizing some proper STF coding and modulations, STF coded MIMO systems can exploit all of the spatial, temporal and frequency diversities, hence promise to yield remarkable performance improvement.

Currently, UWB technology achieves data rates ranging from 55 Mb/s to 480 Mb/s over distances up to 10 meters. To

enhance the data rates and the coverage ranges, the application of MIMO scheme to UWB has gained considerable interest recently. To this date, multi-antenna UWB technology has been well documented for the traditional single-band UWB system [4]. On the other hand, research for multi-antenna multiband UWB is still largely unexplored, thus offering limited resources in handling the benefits and challenges of UWB-MIMO communications.

In this paper, we propose a general framework to characterize the performance of UWB-MIMO systems with multiband OFDM. A combination of STF coding and hopping multiband UWB transmission is proposed to exploit all of the available spatial and frequency diversities. In the performance evaluation, we do not impose any restriction on the delays or the average powers of the multipath components, and the proposed framework is applicable for any channel models. Since Nakagami- $m$  statistics can be used to model a wide range of fading conditions, we evaluate the theoretical performances of UWB systems by using the tap-delay line Nakagami- $m$  fading model, as it can provide some insightful understanding of UWB systems. We quantify the average pairwise error probability as well as the diversity and the coding advantages, regardless of specific coding schemes. Simulation results confirm the theoretical expectation of considerable performance improvement, gained from adopting STF codes in multiband system.

The rest of the paper is organized as follows. In Section II, we present the multiband UWB-MIMO system model, including the signal modulation, channel model, receiver description, and detection technique. The performance analysis of a peer-to-peer multiband UWB-MIMO system is presented in Section III. Section IV shows simulation results, and finally Section V concludes the paper.

## II. MULTIBAND UWB-MIMO SYSTEM MODEL

Consider a multiband OFDM scenario that has been proposed in the IEEE 802.15.3a WPAN standard [5]. The available UWB spectrum of 7.5 GHz is divided into several subbands, each with bandwidth  $BW$  of at least 500 MHz. Each user utilizes one subband per transmission. For each user, signals from all transmit antennas share the same subband. Within each subband, OFDM modulation with  $N$  subcarriers is used at each transmit antenna. Different bit rates are achieved by using different channel coding, frequency spreading, or time spreading rates. We consider a multiband system with fast band-hopping rate, i.e., the signal is transmitted on a subband during one OFDM symbol interval, then moved to a different subband at the next interval.

### A. Transmitter Description

We consider a peer-to-peer multiband UWB system with  $N_t$  transmit and  $N_r$  receive antennas, as shown in Fig. 1. The

<sup>1</sup>This work was supported in part by U.S. Army Research Laboratory under Cooperative Agreement DAAD 190120011.

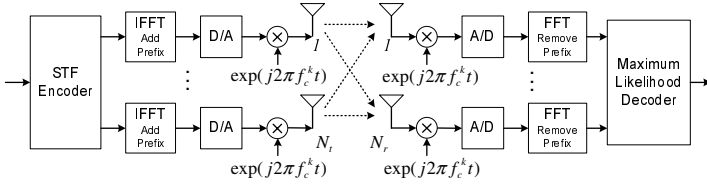


Fig. 1: Multiband UWB-MIMO system.

information is encoded across  $N_t$  transmit antennas,  $N$  OFDM subcarriers, and  $K$  OFDM blocks.

At the transmitter, the coded information sequence from a channel encoder is partitioned into blocks of  $N_b$  bits. Each block is mapped onto a  $KN \times N_t$  STF codeword matrix

$$\mathbf{D} = [ \mathbf{D}_0^T \quad \mathbf{D}_1^T \quad \cdots \quad \mathbf{D}_{K-1}^T ]^T, \quad (1)$$

where

$$\mathbf{D}_k = [ \mathbf{d}_1^k \quad \mathbf{d}_2^k \quad \cdots \quad \mathbf{d}_{N_t}^k ], \quad (2)$$

in which  $\mathbf{d}_i^k = [d_i^k(0) \quad d_i^k(1) \quad \cdots \quad d_i^k(N-1)]^T$  for  $i = 1, 2, \dots, N_t$  and  $k = 0, 1, \dots, K-1$ . The symbol  $d_i^k(n)$ ,  $n = 0, 1, \dots, N-1$ , represents the complex symbol to be transmitted over subcarrier  $n$  by transmit antenna  $i$  during the  $k^{\text{th}}$  OFDM symbol period. The matrix  $\mathbf{D}$  is normalized to have average energy  $\mathbb{E}[\|\mathbf{D}\|^2] = KNN_t$ , where  $\|\cdot\|$  denotes the Frobenius norm. At the  $k^{\text{th}}$  OFDM block, the transmitter applies  $N$ -point IFFT over each column of the matrix  $\mathbf{D}_k$ , yielding an OFDM symbol of length  $T_{FFT}$ .

The IFFT output is added with a cyclic prefix of length  $T_{CP}$  and a guard interval of duration  $T_{GI}$ , and then passed through a digital-to-analog converter, resulting in an analog baseband OFDM signal of duration  $T_{SYM} = T_{FFT} + T_{CP} + T_{GI}$ . The baseband OFDM signal to be transmitted by the  $i^{\text{th}}$  transmit antenna at the  $k^{\text{th}}$  OFDM block can be expressed as

$$x_i^k(t) = \sqrt{\frac{E}{N_t}} \sum_{n=0}^{N-1} d_i^k(n) \exp\{j2\pi n \Delta f (t - T_{CP})\} \quad (3)$$

for  $t \in [T_{CP}, T_{FFT} + T_{CP}]$ . In (3),  $\mathbf{j} \triangleq \sqrt{-1}$ , and  $\Delta f = 1/T_{FFT} = BW/N$  is the frequency separation between two adjacent subcarriers. The factor  $\sqrt{E/N_t}$  guarantees that the average energy per transmitted symbol is  $E$ , independent of the number of transmit antennas.

The complex baseband signal  $x_i^k(t)$  is filtered, up-converted to an RF signal with a carrier frequency  $f_c^k$ , and finally sent from the  $i^{\text{th}}$  transmit antenna. The transmitted multiband UWB signal at transmit antenna  $i$  over  $K$  OFDM symbol periods is given by

$$s_i(t) = \sum_{k=0}^{K-1} \text{Re} \{ x_i^k(t - k T_{SYM}) \exp(j2\pi f_c^k t) \}.$$

The carrier frequency  $f_c^k$  specifies the subband, in which the signal is transmitted during the  $k^{\text{th}}$  OFDM symbol period. The carrier frequency can be changed from one OFDM block to another, so as to enable the frequency diversity while minimize the multiple access interference. Note that  $f_c^k$  is the same for every transmit antenna, and the transmissions from all of the  $N_t$  transmit antennas are simultaneous and synchronous. Since  $N_b$  information bits are transmitted in  $KT_{SYM}$  seconds, the transmission rate (without channel coding) is  $R = N_b/(KT_{SYM})$ .

## B. Channel Model

We consider frequency-selective fading channel [6], which is modeled as a tapped-delay line with  $L$  taps. At the  $k^{\text{th}}$  OFDM block, the channel impulse response from the  $i^{\text{th}}$  transmit antenna to the  $j^{\text{th}}$  receive antenna can be described as

$$h_{ij}^k(t) = \sum_{l=0}^{L-1} \alpha_{ij}^k(l) \delta(t - \tau_l), \quad (4)$$

where  $\alpha_{ij}^k(l)$  is the multipath gain coefficient,  $L$  denotes the number of resolvable paths, and  $\tau_l$  represents the path delay of the  $l^{\text{th}}$  path. The measurements in UWB channels indicate that the amplitude of each path follows either a log-normal or Nakagami- $m$  distribution [7]. The advantage of Nakagami- $m$  statistics is that they can model a wide range of fading conditions by adjusting their fading parameters. In fact, Nakagami- $m$  distributions with large value  $m$  are similar to the log-normal distributions. Therefore, we will assume that the amplitude of the  $l^{\text{th}}$  path,  $|\alpha_{ij}^k(l)|$ , is modeled as a Nakagami- $m$  random variable [8] with fading parameter  $m$  and average power  $\Omega_l = \mathbb{E}[|\alpha_{ij}^k(l)|^2]$ . The powers of the  $L$  paths are normalized such that  $\sum_{l=0}^{L-1} \Omega_l = 1$ . We assume that the time delay  $\tau_l$  and the average power  $\Omega_l$  are the same for every transmit-receive link.

## C. Receiver Processing

The signal received at each receive antenna is a superposition of the  $N_t$  transmitted signals corrupted by additive white Gaussian noise. Assume that the receiver perfectly synchronizes to the band switching pattern. The received RF signal at each receive antenna is down-converted to a complex baseband signal, matched to the pulse waveform, and then sampled before passing through an OFDM demodulator. After the OFDM demodulator discards the cyclic prefix and performs an  $N$ -point FFT, a maximum-likelihood detection is jointly performed across all  $N_r$  receive antennas. The choice of prefix length greater than the duration of the channel impulse response ensures that the interference between OFDM symbols is eliminated. Effectively, the frequency-selective fading channel decouples into a set of  $N$  parallel frequency-nonselective fading channels, whose fading coefficients are equal to the channel frequency response at the center frequency of the subcarriers. Therefore, the received signal at the  $n^{\text{th}}$  subcarrier at receive antenna  $j$  during OFDM block  $k$  can be expressed as

$$y_j^k(n) = \sqrt{\frac{E}{N_t}} \sum_{i=1}^{N_t} d_i^k(n) H_{ij}^k(n) + z_j^k(n), \quad (5)$$

where

$$H_{ij}^k(n) = \sum_{l=0}^{L-1} \alpha_{ij}^k(l) \exp[-j2\pi n \Delta f \tau_l] \quad (6)$$

is the frequency response of the channel at subcarrier  $n$  between the  $i^{\text{th}}$  transmit and the  $j^{\text{th}}$  receive antenna during the  $k^{\text{th}}$  OFDM block. In (5),  $z_j^k(n)$  represents the noise sample, which is modeled as complex Gaussian random variable with zero mean and a two-sided power spectral density of  $N_0/2$ .

For subsequent performance evaluation, we rewrite the received signal (see (5)) at receive antenna  $j$  in the matrix form as

$$\mathbf{Y}_j = \sqrt{\frac{E}{N_t}} \mathbf{S}_D \mathbf{H}_j + \mathbf{Z}_j, \quad (7)$$

where  $\mathbf{S}_D$  is a  $KN \times KN N_t$  data matrix of a form

$$\mathbf{S}_D = [\mathbf{S}_1 \quad \mathbf{S}_2 \quad \cdots \quad \mathbf{S}_{N_t}], \quad (8)$$

in which  $\mathbf{S}_i$  is a  $KN \times KN$  diagonal matrix whose main diagonal comprises the information to be sent from transmit antenna  $i$ . We format  $\mathbf{S}_i$  as

$$\mathbf{S}_i = \text{diag} \left( [(\mathbf{d}_i^0)^T (\mathbf{d}_i^1)^T \cdots (\mathbf{d}_i^{K-1})^T]^T \right),$$

where  $\text{diag}(\mathbf{x})$  is a diagonal matrix with the elements of  $\mathbf{x}$  on its main diagonal. The  $KN N_t \times 1$  channel vector  $\mathbf{H}_j$  is of a form

$$\mathbf{H}_j = [\mathbf{H}_{1j}^T \quad \mathbf{H}_{2j}^T \quad \cdots \quad \mathbf{H}_{N_t j}^T]^T, \quad (9)$$

$$\mathbf{H}_{ij} = [H_{ij}^0(0) \cdots H_{ij}^0(N-1) \cdots H_{ij}^{K-1}(0) \cdots H_{ij}^{K-1}(N-1)]^T.$$

The received signal vector  $\mathbf{Y}_j$  of size  $KN N_r \times 1$  is given by  $\mathbf{Y}_j = [(\mathbf{y}_j^0)^T (\mathbf{y}_j^1)^T \cdots (\mathbf{y}_j^{K-1})^T]^T$ , in which  $\mathbf{y}_j^k$  is an  $N \times 1$  vector whose  $n^{\text{th}}$  element is  $y_j^k(n)$ . The noise vector  $\mathbf{Z}$  has the same form as  $\mathbf{Y}$  by replacing  $y_j^k(n)$  with  $z_j^k(n)$ .

We assume that the receiver has perfect knowledge of the channel state information, while the transmitter has no channel information. The receiver exploits a maximum likelihood decoder, where the decoding process is jointly performed on  $N_r$  receive signal vectors. The decision rule can be stated as

$$\hat{\mathbf{D}} = \arg \min_{\mathbf{D}} \sum_{j=1}^{N_r} \|\mathbf{Y}_j - \sqrt{\frac{E}{N_t}} \mathbf{S}_D \mathbf{H}_j\|^2.$$

### III. PERFORMANCE ANALYSIS

In this section, we present a general framework to analyze the performance of multi-antenna multiband UWB system. We derive the performance of STF coded multiband UWB systems in terms of pairwise error probability (PEP). Suppose that  $\Delta_S \triangleq \mathbf{S}_D - \mathbf{S}_{\hat{D}}$  is the difference between two data matrices,  $\mathbf{S}_D$  and  $\mathbf{S}_{\hat{D}}$ , which are related to two distinct STF codewords  $\mathbf{D}$  and  $\hat{\mathbf{D}}$ , respectively. Following the computation steps as in [6], the PEP conditioned on the channel matrix is given by

$$P_e | \mathbf{H}_j = Q \left( \sqrt{\frac{\rho}{2N_t} \sum_{j=1}^{N_r} \|\Delta_S \mathbf{H}_j\|^2} \right) \quad (10)$$

where  $\rho = E/N_0$  is the average signal-to-noise ratio (SNR) at each receive antenna, and  $Q(x)$  is the Gaussian error function,  $Q(x) = \frac{1}{\sqrt{2\pi}} \int_x^\infty \exp(-\frac{s^2}{2}) ds$ . The average PEP can be obtained by calculating the expected value of the conditional PEP with respect to the distribution of  $\gamma \triangleq \sum_{j=1}^{N_r} \|\Delta_S \mathbf{H}_j\|^2$ , i.e.,

$$P_e = \int_0^\infty Q \left( \sqrt{\frac{\rho}{2N_t} s} \right) p_\gamma(s) ds, \quad (11)$$

where  $p_\gamma(s)$  is the probability density function (PDF) of  $\gamma$ .

For convenience, let us denote an  $N_t N_r L K \times 1$  channel vector

$$\mathbf{a} = [\mathbf{a}_1^T \quad \mathbf{a}_2^T \quad \cdots \quad \mathbf{a}_{N_r}^T]^T,$$

where  $\mathbf{a}_j$  contains the multipath gains from all transmit antennas to the  $j^{\text{th}}$  receive antenna. The  $N_t L K \times 1$  vector  $\mathbf{a}_j$  is

$$\mathbf{a}_j = [(\mathbf{a}_{1j}^0)^T \cdots (\mathbf{a}_{N_t j}^0)^T \cdots (\mathbf{a}_{1j}^{K-1})^T \cdots (\mathbf{a}_{N_t j}^{K-1})^T]^T \quad (12)$$

in which

$$\mathbf{a}_{ij}^k = [\alpha_{ij}^k(0) \quad \alpha_{ij}^k(1) \quad \cdots \quad \alpha_{ij}^k(L-1)]^T. \quad (13)$$

According to (6) and (12), we can express (9) as

$$\mathbf{H}_j = (\mathbf{I}_{KN_t} \otimes \mathbf{W}) \mathbf{a}_j,$$

where  $\otimes$  denotes the Kronecker product,  $\mathbf{I}_M$  represents an  $M \times M$  identity matrix, and  $\mathbf{W}$  is an  $N \times L$  Fourier matrix whose  $(n, l)^{\text{th}}$  component is  $\exp(-j2\pi n \Delta f \tau_l)$ . As a consequence,  $\gamma$  can be expressed as

$$\gamma = \sum_{j=1}^{N_r} \|\Delta_S (\mathbf{I}_{KN_t} \otimes \mathbf{W}) \mathbf{a}_j\|^2. \quad (14)$$

We can see from (14) that the distribution of  $\gamma$  depends on the joint distribution of the multipath gain coefficients,  $\alpha_{ij}^k(l)$ .

In the sequel, we first analyze the performance of multiband UWB-MIMO system with independent fading. Such assumption allows us to characterize the performances of UWB systems with the diversity and the coding advantages. Then, we investigate the performance of a more realistic system, where the multipath gain coefficients are allowed to be correlated.

#### A. Independent Fading

Due to the band hopping, the  $K$  OFDM symbols in each STF codeword are sent over different subbands. With an ideal band hopping, we assume that the signal transmitted over  $K$  different subbands undergo independent fading. We also assume that the path gains  $\alpha_{ij}^k(l)$  are independent for different paths and different transmit-receive links, and each transmit-receive link has the same power delay profile, i.e.,  $E[|\alpha_{ij}^k(l)|^2] = \Omega_l$ . The correlation matrix of  $\mathbf{a}_j$  is given by

$$E[\mathbf{a}_j \mathbf{a}_j^{\mathcal{H}}] = \mathbf{I}_{KN_t} \otimes \mathbf{\Omega}, \quad (15)$$

where  $(\cdot)^{\mathcal{H}}$  denotes conjugate transpose operation, and  $\mathbf{\Omega} = \text{diag}(\Omega_0, \Omega_1, \cdots, \Omega_{L-1})$  is an  $L \times L$  matrix formed from the power of the  $L$  paths.

Denote  $\mathbf{\Omega}^{\frac{1}{2}} = \text{diag}(\sqrt{\Omega_0}, \sqrt{\Omega_1}, \cdots, \sqrt{\Omega_{L-1}})$ , and let  $\mathbf{q}_j = (\mathbf{I}_{KN_t} \otimes \mathbf{\Omega}^{\frac{1}{2}})^{-1} \mathbf{a}_j$ . We can show that the elements of  $\mathbf{q}_j$  are identically independent distributed (iid) Nakagami- $m$  random variables with normalized power  $\Omega = 1$ . Substitute  $\mathbf{a}_j = (\mathbf{I}_{KN_t} \otimes \mathbf{\Omega}^{\frac{1}{2}}) \mathbf{q}_j$  into (14), and apply the property of Kronecker product ([9] p.251), resulting in

$$\gamma = \sum_{j=1}^{N_r} \|\Delta_S (\mathbf{I}_{KN_t} \otimes \mathbf{W} \mathbf{\Omega}^{\frac{1}{2}}) \mathbf{q}_j\|^2 = \sum_{j=1}^{N_r} \mathbf{q}_j^{\mathcal{H}} \mathbf{\Psi} \mathbf{q}_j, \quad (16)$$

where  $\mathbf{\Psi} = (\mathbf{I}_{KN_t} \otimes \mathbf{W} \mathbf{\Omega}^{\frac{1}{2}})^{\mathcal{H}} \Delta_S^{\mathcal{H}} \Delta_S (\mathbf{I}_{KN_t} \otimes \mathbf{W} \mathbf{\Omega}^{\frac{1}{2}})$ . Since  $\mathbf{\Psi}$  is a Hermitian matrix of size  $KN_t L \times KN_t L$ , it can be decomposed into  $\mathbf{\Psi} = \mathbf{V} \mathbf{\Lambda} \mathbf{V}^{\mathcal{H}}$ , where  $\mathbf{V} \triangleq [\mathbf{v}_1 \cdots \mathbf{v}_{KN_t L}]$  is a unitary matrix, and  $\mathbf{\Lambda} = \text{diag}\{\lambda_1(\mathbf{\Psi}), \dots, \lambda_{KN_t L}(\mathbf{\Psi})\}$  is a diagonal matrix whose diagonal elements are the eigenvalues of  $\mathbf{\Psi}$ . After some manipulations, we arrive at

$$\gamma = \sum_{j=1}^{N_r} \sum_{n=1}^{KN_t L} \lambda_n(\mathbf{\Psi}) |\beta_{j,n}|^2, \quad (17)$$

where  $\beta_{j,n} \triangleq \mathbf{v}_n^H \mathbf{q}_j$ . Since  $\mathbf{V}$  is unitary and components of  $\mathbf{q}_j$  are iid,  $\beta_{j,n}$ 's are independent random variables, whose magnitudes are approximately Nakagami- $\tilde{m}$  distributed with ([8] p.25)

$$\tilde{m} = (KLN_t m)/(KLN_t m - m + 1) \quad (18)$$

and average power  $\Omega = 1$ . Hence, the PDF of  $|\beta_{j,n}|^2$  approximately follows Gamma distribution. Now, the average PEP can be obtained by substituting (17) into (10), and averaging (10) with respect to the distribution of  $|\beta_{j,n}|^2$ . To this end, we resort to an alternate representation of Q function,  $Q(x) = \frac{1}{\pi} \int_0^{\pi/2} \exp(-\frac{x^2}{2\sin^2\theta}) d\theta$  for  $x \geq 0$ . This allows us to express (10) in term of moment generating function (MGF) of  $\gamma$ , denoted by  $\phi_\gamma(s)$ . Due to the fact that  $\phi_{|\beta_{j,n}|^2}(s) = (1 - \frac{\Omega}{\tilde{m}}s)^{-\tilde{m}}$ , and  $|\beta_{j,n}|^2$  are independent, the average PEP is given by

$$P_e = \frac{1}{\pi} \int_0^{\pi/2} \prod_{n=1}^{KLN_t} \left( 1 + \frac{\rho(\Omega/\tilde{m})}{4N_t \sin^2\theta} \lambda_n(\Psi) \right)^{-\tilde{m}N_r} d\theta.$$

By bounding the PEP above with  $\theta = \pi/2$  and assuming high SNR, we arrive at the upper bound of the PEP:

$$P_e \leq \left[ \prod_{n=1}^{rank(\Psi)} \left( \frac{\rho}{4N_t} \frac{\Omega}{\tilde{m}} \lambda_n(\Psi) \right) \right]^{-\tilde{m}N_r}, \quad (19)$$

where  $rank(\Psi)$  is the rank and  $\{\lambda_n(\Psi)\}_{n=1}^{rank(\Psi)}$  are nonzero eigenvalues of matrix  $\Psi$ . From (19), we can quantify the performance of STF coded multiband UWB with the diversity gain  $G_d = \min_{\mathbf{D} \neq \mathbf{I}} \tilde{m}N_r rank(\Psi)$ , and the coding gain  $G_c = \min_{\mathbf{D} \neq \mathbf{I}} \frac{\Omega}{\tilde{m}} \left( \prod_{n=1}^{rank(\Psi)} \lambda_n(\Psi) \right)^{1/rank(\Psi)}$ .

In order to specify the maximum achievable diversity gain, we calculate the rank of  $\Psi$  as follows. According to (16) and the rank property, we have  $rank(\Psi) = rank(\Delta_S(\mathbf{I}_{KN_t} \otimes \mathbf{W}\Omega^{1/2}))$ . Observe that the size of  $\Delta_S$  is  $KN \times KNN_t$ , whereas the size of  $\mathbf{W}\Omega^{1/2}$  is  $N \times L$ . Therefore, the rank of matrix  $\Psi$  becomes  $rank(\Psi) \leq \min\{KN, KLN_t\}$ . Hence, the maximum achievable diversity gain is

$$G_d^{max} = \min\{\tilde{m}KLN_tN_r, \tilde{m}KNN_r\}. \quad (20)$$

Note that the diversity gain in (20) depends on the parameter  $\tilde{m}$  which is close to one for any fading parameter  $m$ . Indeed, for multiband UWB-MIMO systems,

$$\tilde{m} = (1 - (KLN_t)^{-1} + (KLN_t m)^{-1})^{-1} \approx 1. \quad (21)$$

In this case, the maximum achievable diversity gain is well approximated by

$$G_d^{max} = \min\{KLN_tN_r, KNN_r\}. \quad (22)$$

The result in the analysis above is somewhat surprising since the diversity gain of multiband UWB-MIMO system does not depend on the fading parameter  $m$ . The reason behind this is that  $\beta_{j,n}$  in (17) is a normalized summation of  $KLN_t$  independent Nakagami random variables. When  $KLN_t$  is large enough,  $\beta_{j,n}$  behaves like a complex Gaussian random variable, and hence the channel is like Rayleigh faded. Since the ultra-wide bandwidth results in a large number of multipath components, the effect of  $KLN_t$  on the diversity gain dominates the effect of fading

parameter  $m$ . This implies that the diversity advantage does not depend on the severity of the fading. The diversity gain obtained under Nakagami fading with arbitrary  $m$  parameter is almost the same as that obtained in Rayleigh fading channels.

We emphasize here the major difference between the use of STF coding in the conventional OFDM systems and in the multi-band OFDM systems. For STF coding in the conventional OFDM systems, the symbols are continuously transmitted in the same subband, hence the temporal diversity depends on the time varying nature of the channel [3]. In contrast, the diversity gain in (22) reveals that with band switching, the STF coded multiband UWB is able to achieve the diversity gain of  $\min\{KLN_tN_r, KNN_r\}$ , regardless of the channel time-correlation property.

It is worth noting that the proposed framework incorporates the analysis for ST or SF coded UWB systems as special cases. In case of single-carrier frequency-non-selective channel, i.e.,  $N = 1$  and  $L = 1$ , the performance of STF coded UWB is similar to that of ST coded UWB system. In case of coding within one OFDM block ( $K = 1$ ), the performance of STF coded UWB is the same as that of SF coded scheme. The maximum diversity reduces to  $\min\{LN_tN_r, NN_r\}$ . This reveals that STF coding together with band hopping across  $K$  OFDM blocks can offer the diversity advantage of  $K$  times larger than that of SF coding approach.

### B. Correlated Fading

In case of correlated fading, we express  $\gamma$  in (14) as

$$\gamma = \mathbf{a}^H \left\{ \mathbf{I}_{N_r} \otimes [(\mathbf{I}_{KN_t} \otimes \mathbf{W}^H) \Delta_S^H \Delta_S (\mathbf{I}_{KN_t} \otimes \mathbf{W})] \right\} \mathbf{a}. \quad (23)$$

To simplify the analysis, we assume that the channel correlation matrix,  $\mathbf{R}_A = E[\mathbf{a}\mathbf{a}^H]$  is of full rank. Since  $\mathbf{R}_A$  is positive definite Hermitian symmetric, it has a symmetric square root  $\mathbf{U}$  such that  $\mathbf{R} = \mathbf{U}^H \mathbf{U}$ , where  $\mathbf{U}$  is also of full rank [9]. Let  $\mathbf{q} = \mathbf{U}^{-1} \mathbf{a}$ , then it follows that  $E[\mathbf{q}\mathbf{q}^H] = \mathbf{I}_{KLN_tN_r}$ , i.e., the components of  $\mathbf{q}$  are uncorrelated. Substituting  $\mathbf{a} = \mathbf{U}\mathbf{q}$  into (23), we have  $\gamma = \mathbf{q}^H \Phi \mathbf{q}$  where

$$\Phi = \mathbf{U}^H \left\{ \mathbf{I}_{N_r} \otimes [(\mathbf{I}_{KN_t} \otimes \mathbf{W}^H) \Delta_S^H \Delta_S (\mathbf{I}_{KN_t} \otimes \mathbf{W})] \right\} \mathbf{U}. \quad (24)$$

Accordingly, using an eigenvalue decomposition of the matrix  $\Phi$ , we can express  $\gamma$  as  $\gamma = \sum_{n=1}^{KLN_tN_r} \lambda_n(\Phi) |\beta_n|^2$ , where  $\beta_n \triangleq \mathbf{v}_n^H \mathbf{q}$ ,  $\mathbf{v}_n$ 's and  $\lambda_n(\Phi)$ 's are the eigenvectors and the eigenvalues of matrix  $\Phi$ . From (11), the PEP can be obtained by averaging the conditional PEP with respect to the joint distribution of  $\{|\beta_n|^2\}$ :

$$P_e = \int_0^\infty \cdots \int_0^\infty Q \left( \sqrt{\frac{\rho}{2N_t} \sum_{n=1}^M \lambda_n(\Phi) s_n} \right) \times p_{|\beta_1|^2 \cdots |\beta_M|^2}(s_1, \dots, s_M) ds_1 \cdots ds_M, \quad (25)$$

where  $M = KLN_tN_r$ . In general,  $\beta_n$ 's for different  $n$  are not independent, and the closed-form solution for (25) is difficult, if not possible, to determine. In what follows, we will discuss two special cases where (25) can be further simplified.

#### Special case 1: Constant fading

In case of constant fading over  $K$  OFDM blocks, i.e., the modulated OFDM signal is transmitted continually over the same subband for entire  $K$  OFDM blocks, (14) can be re-expressed as

$$\gamma = \sum_{j=1}^{N_r} \|(\mathbf{C}_D - \mathbf{C}_{\hat{D}}) (\mathbf{I}_{N_t} \otimes \mathbf{W}) \tilde{\mathbf{a}}_j\|^2, \quad (26)$$

where  $\mathbf{C}_D = [\mathbf{C}_0^T \mathbf{C}_1^T \cdots \mathbf{C}_{K-1}^T]^T$  is a  $KN \times N_t N$  matrix, and  $\mathbf{C}_k = [\text{diag}(\mathbf{d}_1^k) \cdots \text{diag}(\mathbf{d}_{N_t}^k)]$ . The channel vector  $\tilde{\mathbf{a}}_j$  of size  $LN_t \times 1$  is given by  $\tilde{\mathbf{a}}_j = [\mathbf{a}_{1j}^T \mathbf{a}_{2j}^T \cdots \mathbf{a}_{N_t j}^T]^T$ , in which  $\mathbf{a}_{ij}$  is defined in (13). Since the path gains  $\mathbf{a}_{ij}^k$ 's are the same for every  $k$ ,  $0 \leq k \leq K-1$ , the time superscript index  $k$  is omitted to simplify the notations. Following the steps given previously, we can show that the average PEP has the same form as (25) with  $M$  replaced by  $LN_t N_r$  and  $\{\lambda_n(\tilde{\Phi})\}_{n=1}^{LN_t N_r}$  being the eigenvalues of

$$\tilde{\Phi} = \tilde{\mathbf{U}}^H \{ \mathbf{I}_{N_r} \otimes [(\mathbf{I}_{N_t} \otimes \mathbf{W}^H) \Delta_C^H \Delta_C (\mathbf{I}_{N_t} \otimes \mathbf{W})] \} \tilde{\mathbf{U}}.$$

Here,  $\Delta_C \triangleq \mathbf{C}_D - \mathbf{C}_{\hat{D}}$  and  $\tilde{\mathbf{U}}$  is a symmetric square root of  $\tilde{\mathbf{R}}_A = \mathbb{E}[\tilde{\mathbf{a}}\tilde{\mathbf{a}}^H]$ , in which  $\tilde{\mathbf{a}} = [\tilde{\mathbf{a}}_1^T \tilde{\mathbf{a}}_2^T \cdots \tilde{\mathbf{a}}_{N_r}^T]^T$ .

With a further assumption that the path gains are independent for every transmit-receive link, the average PEP can be obtained in a similar fashion to that derived in Section III-A as

$$P_e \leq \left[ \prod_{n=1}^{\text{rank}(\Theta)} \left( \frac{\rho}{4N_t} \frac{\Omega}{\tilde{m}} \lambda_n(\Theta) \right) \right]^{-\tilde{m}N_r}, \quad (27)$$

where  $\lambda_n(\Theta)$ 's are the nonzero eigenvalues of the matrix  $\Theta = (\mathbf{I}_{N_t} \otimes \mathbf{W}^H) \Delta_C^H \Delta_C (\mathbf{I}_{N_t} \otimes \mathbf{W})$ . Observe that the maximum rank of  $\Delta_C (\mathbf{I}_{N_t} \otimes \mathbf{W})$  is  $\min\{LN_t, KN\}$ . Hence, the maximum achievable diversity gain becomes

$$G_d^{max} = \min\{\tilde{m}LN_t N_r, \tilde{m}KN N_r\}. \quad (28)$$

Since  $KN$  is typically larger than  $LN_t$ , we can conclude from (28) that when  $K$  OFDM symbols are sent on one subband prior to band switching, coding across  $K$  OFDM blocks does not offer any additional diversity advantage compared to the coding scheme within one OFDM block.

**Special case 2: Fading parameter  $m = 1$**

With  $m = 1$ , Nakagami is equivalent to Rayleigh distribution, and the path gain coefficients can be modeled as complex Gaussian random variables. Recall that for Gaussian random variables, uncorrelated implies independent. Thus,  $\{|\beta_n|^2\}$  in (25) becomes a set of iid Rayleigh random variables. By the use of MGF of  $\gamma$ , the average PEP in (25) is given by

$$P_e = \frac{1}{\pi} \int_0^{\pi/2} \prod_{n=1}^{KN_t N_r} \left( 1 + \frac{\rho}{4N_t \sin^2 \theta} \lambda_n(\Phi) \right)^{-1} d\theta,$$

where  $\Phi$  is defined in (24). The PEP above can be bounded by

$$P_e \leq \left[ \prod_{n=1}^{KN_t N_r} \left( \frac{\rho}{4N_t} \lambda_n(\Phi) \right) \right]^{-1}$$

at high SNR. Therefore, the performance of this system can be quantified as the diversity gain:  $G_d = \min_{\mathbf{D} \neq \hat{\mathbf{D}}} N_r \text{rank}(\Phi)$ , and the coding gain:  $G_c = \min_{\mathbf{D} \neq \hat{\mathbf{D}}} \left( \prod_{n=1}^{\text{rank}(\Phi)} \lambda_n(\Phi) \right)^{\frac{1}{\text{rank}(\Phi)}}$ .

#### IV. SIMULATION RESULTS

We performed simulations for multi-antenna multiband UWB systems with  $N = 128$  subcarriers and the subband bandwidth of  $BW = 528$  MHz. The OFDM symbol is of duration  $T_{FFT} = 242.42$  ns. After adding the cyclic prefix of length  $T_{CP} = 60.61$  ns and the guard interval of length  $T_{GI} = 9.47$  ns, the symbol duration becomes  $T_{SYM} = 312.5$  ns. Our simulated

channel model is based on (4) with the path amplitudes  $|\alpha_{ij}^k(l)|$  being independent Nakagami- $m$  random variables and the phases  $\angle \alpha_{ij}^k(l)$  being uniform over  $[0, 2\pi)$ . The power delay profile, used to specify the path delays  $\tau_l$ 's and powers  $\Omega_l$ 's, follows the statistical model in [10]. In our simulations, the STF codeword  $\mathbf{D} = [\mathbf{D}_0^T \mathbf{D}_1^T \cdots \mathbf{D}_{K-1}^T]^T$  in (1) is further simplified as

$$\mathbf{D}_k = \left[ \mathbf{G}_{k,1}^T \quad \mathbf{G}_{k,2}^T \quad \cdots \quad \mathbf{G}_{k,P}^T \quad \mathbf{0}_{(N-P\Upsilon N_t) \times N_t}^T \right],$$

in which  $\Upsilon$  is a fixed integer between 1 and  $L$ ,  $P = \lfloor N/(\Upsilon N_t) \rfloor$ , and  $\mathbf{0}_{m \times n}$  stands for an  $m \times n$  all-zero matrix. The  $\Upsilon N_t \times N_t$  code matrices  $\{\mathbf{G}_{k,p}\}_{k=0}^{K-1}$  for each  $p$  are jointly designed, whereas the matrices  $\mathbf{G}_{k,p}$  and  $\mathbf{G}_{k',p'}$  with  $p \neq p'$  are designed independently. Such code structures are able to provide the maximum achievable diversity, while enable low computational complexity [3].

Let us consider a system with two transmit antennas. Based on the repetition STF code in [3],  $\mathbf{G}_{k,p}$  is given by

$$\mathbf{G}_{k,p} = (\mathbf{I}_{N_t} \otimes \mathbf{1}_{\Upsilon \times 1}) \begin{pmatrix} x_{p,1} & x_{p,2} \\ -x_{p,2}^* & x_{p,1}^* \end{pmatrix},$$

where  $\mathbf{1}_{m \times n}$  denotes an  $m \times n$  all-one matrix, and  $x_{p,i}$ 's are selected from BPSK or QPSK constellations. Note that  $\mathbf{G}_{k,p}$  is the same for all  $k$ 's. We also use a full-rate STF code with [3]

$$\mathbf{G}_{k,p} = \sqrt{N_t} \begin{pmatrix} \mathbf{x}_{p,1}^k & \mathbf{0}_{\Upsilon \times 1} \\ \mathbf{0}_{\Upsilon \times 1} & \mathbf{x}_{p,2}^k \end{pmatrix},$$

where  $\mathbf{x}_{p,i}^k$  is a  $\Upsilon \times 1$  matrix whose elements are specified as follows. Omitting subscript  $p$  and denoting  $\mathcal{L} = K\Upsilon N_t$ , the  $1 \times \mathcal{L}$  matrix  $\mathbf{x} \triangleq [(\mathbf{x}_1^0)^T (\mathbf{x}_2^0)^T \cdots (\mathbf{x}_1^{K-1})^T (\mathbf{x}_2^{K-1})^T]$  is given by  $\mathbf{x} = (1/\sqrt{K})\mathbf{s}\mathbf{V}(\theta_1, \theta_2, \dots, \theta_{\mathcal{L}})$ , in which  $\mathbf{s} = [s_1 \ s_2 \ \cdots \ s_{\mathcal{L}}]$  is a vector of BPSK or QPSK symbols, and  $\mathbf{V}$  is a Vandermonde matrix with  $\theta_l = e^{j(4l-3)\pi/(2\mathcal{L})}$  for  $\mathcal{L} = 2^s (s \geq 1)$  and  $\theta_l = e^{j(6l-1)\pi/(3\mathcal{L})}$  for  $\mathcal{L} = 2^s \cdot 3^t (s \geq 0, t \geq 1)$ .

First, we consider the performance of coding approach over one OFDM block ( $K = 1$ ). We utilize both repetition and full-rate codes, each with spectral efficiency of 1 bit/s/Hz (omitting the prefix and guard interval) and the data rate (without channel coding) of 409.6 Mbits/s. Fig. 2 depicts the performances of the STF coded UWB system with  $\Upsilon = 2$ . We observe that regardless of particular coding scheme, the spatial diversity gained from multi-antenna architecture does improve the system performance significantly. In addition, the performance can be further improved with the choice of STF codes and permutation schemes. In Fig. 3, we compare the performance of multiband UWB system with different frequency diversity orders. Here, we employ the full-rate code with  $\Upsilon = 2, 3$ , and 4. We can see that by increasing the number of jointly encoded subcarriers, the system performance can be improved. This observation is in accordance with our theoretical result in (19). Therefore, with a properly designed STF code, we can effectively exploit both spatial and frequency diversities in UWB environment.

Second, we compare the performances of STF coded multiband UWB system with fast band-hopping rate and time spreading factors,  $K = 1, 2$ . Fig. IV shows the performances of full-rate STF codes with  $\Upsilon = 2$  and spectral efficiency of 1 bit/s/Hz. It is apparent that the diversity advantage increases with the number of jointly encoded OFDM blocks. Such achieved improvement results from the band hopping rather than the temporal diversity,

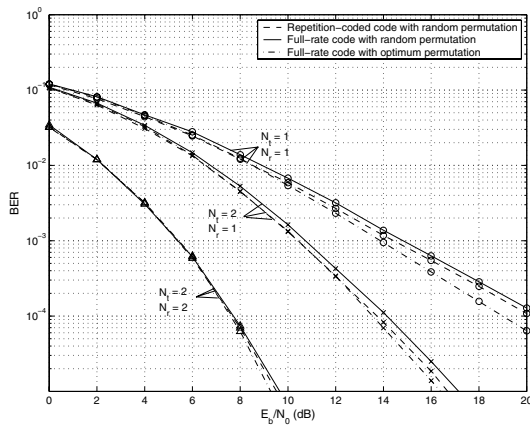


Fig. 2: Performance of multiband UWB with different codes ( $K = 1$ ).

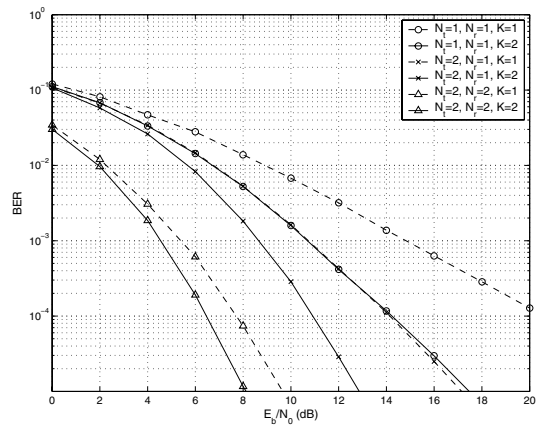


Fig. 4: Performance of multiband with different time spreading factors.

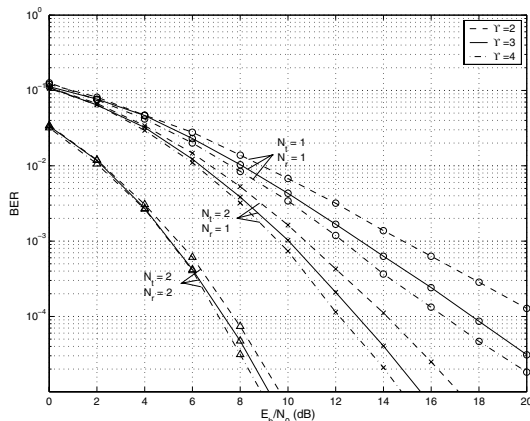


Fig. 3: Performance of multiband UWB with different diversity orders.

and hence the diversity order increases significantly regardless of the temporal correlation of the channel. This supports our analytical results in Section III-A that the diversity order of STF coded multiband UWB with fast hopping rate increases with  $K$ .

Finally, we compare the performance of multiband systems with different band-hopping rates. Fig. 5 depicts the performance of full-rate STF coded UWB system with  $\Upsilon = 2$  and  $K = 2$ . We observe the performance degradation when the band-hopping rate decreases, which corresponds to the results in (19) and (27) that coding over multiple OFDM blocks will offer the additional diversity advantage when the STF coding is applied together with fast band-hopping scheme, i.e., the  $K$  OFDM symbols in each STF codeword are transmitted on various frequency-bands.

## V. CONCLUSIONS

In this paper, we proposed a multiband MIMO coding framework for UWB systems. By a technique of band hopping in combination with jointly coding across spatial, temporal and frequency domains, our scheme is able to exploit all available spatial and multipath diversities, richly inherent in UWB environments. We showed that the maximum achievable diversity advantage of our proposed system is  $KLN_tN_r$  regardless of the temporal correlation of the channel. An interesting result is that the diversity advantage obtained under Nakagami fading with arbitrary  $m$  parameter is almost the same as that obtained in Rayleigh fading channels. Simulation results showed that the employment of STF coding and band hopping techniques is able

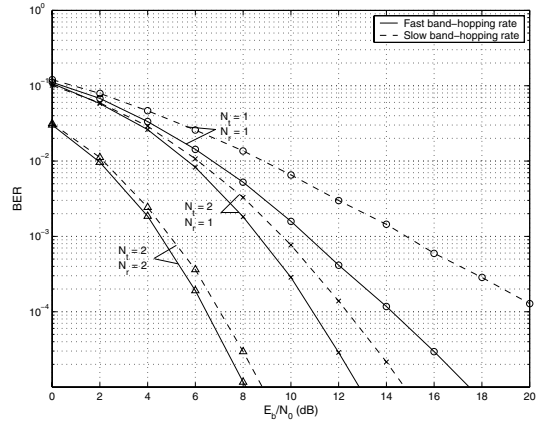


Fig. 5: Performance of multiband UWB with different hopping rates.

to increase the diversity order significantly, thereby considerably improving system performance. In case of single-antenna system, increasing the number of jointly encoded OFDM blocks from one to two yields the performance improvement of 6 dB at a BER of  $10^{-4}$ . By increasing also the number of transmit antennas from one to two, the proposed STF coded multiband UWB system has a total gain of 9 dB at a BER of  $10^{-4}$ .

## REFERENCES

- [1] A. Batra, et. al, "Multi-Band OFDM Physical Layer Proposal for IEEE 802.15 Task Group 3a," IEEE P802.15-03/268r3, Mar. 2004.
- [2] W. Su, Z. Safar, and K. J. R. Liu, "Full-Rate Full-Diversity Space-Frequency Codes with Optimum Coding Advantage," *IEEE Trans. on Inform. Theory*, to appear in vol. 51, no. 1, Jan. 2005.
- [3] W. Su, Z. Safar, and K. J. R. Liu, "Towards Maximum Achievable Diversity in Space, Time and Frequency: Performance Analysis and Code Design," *IEEE Trans. on Wireless Commun.*, to appear.
- [4] W. P. Siriwoongpairat, M. Olfat, and K. J. R. Liu, "Performance Analysis and Comparison of Time Hopping and Direct Sequence UWB-MIMO Systems," *EURASIP J. on Applied Signal Proc.*, to appear in Dec. 2004.
- [5] IEEE 802.15WPAN High Rate Alternative PHY Task Group 3a (TG3a). Internet: [www.ieee802.org/15/pub/TG3a.html](http://www.ieee802.org/15/pub/TG3a.html)
- [6] J. G. Proakis, *Digital Communications*, McGraw-Hill, New York, 2001.
- [7] A. F. Molisch, J. R. Foerster, and M. Pendergrass, "Channel Models for Ultrawideband Personal Area Networks," *IEEE Wireless Commun.*, vol. 10, no. 6, pp. 14-21, Dec. 2003.
- [8] M. Nakagami, "The m-Distribution: A General Formula of Intensity Distribution of Rapid Fading," *Statistical Methods in Radio Wave Propagation*, W. G. Hoffman, Ed. Oxford, England: Pergamon, 1960.
- [9] R. A. Horn and C. R. Johnson, *Matrix Analysis*, Cambridge Univ. Press, New York, 1985.
- [10] S. S. Ghassemzadeh, L. J. Greenstein, T. Sveinsson, and V. Tarokh, "A Multipath Intensity Profile Model for Residential Environments," *IEEE Wireless Commun. and Networking Conf.*, vol. 1, pp. 150-155, Mar. 2003.